

Effect of Kinematic Parameters on MPC based On-line Motion Planning for an Articulated Vehicle

Thaker Nayl, George Nikolakopoulos and Thomas Gustafsson

*Control Engineering Group
Department of Computer Science, Electrical and Space Engineering
Luleå University of Technology
Luleå, Sweden*

Abstract

The aim of this article is to analyze the effect of kinematic parameters on a novel proposed on-line motion planning algorithm for an articulated vehicle based on Model Predictive Control. The kinematic parameters that are going to be investigated are the vehicle's velocity, the maximum allowable change in the articulated steering angle, the safety distance from the obstacles and the total number of obstacles in the operating arena. The proposed modified path planning algorithm for the articulated vehicle belongs to the family of Bug-Like algorithms and is able to take under consideration, the mechanical and physical constraints of the articulated vehicle, as well as its full kinematic model. During the on-line motion planning algorithm, the MPC controller controls the lateral motion of the vehicle, through the rate of the articulation angle, while driving it accurately and safely over the on-line formulated desired path. The efficiency of the proposed combined path planning and control scheme is being evaluated under numerous simulated test cases, while exhaustive simulations have been made for analyzing the dependency of the proposed framework on the kinematic parameters.

Keywords: Model predictive control, articulated vehicle, path planning, collision avoidance.

[☆]Thaker Nayl, George Nikolakopoulos and Thomas Gustafsson are with Luleå University of Technology, Department of Computer, Electrical and Space Engineering, Control Engineering Group, Luleå SE-971 87 Sweden, Corresponding Author Email: thanay@ltu.se

1. Introduction

In general path planning and obstacle avoidance algorithms, coupled with control schemes, are one of the major areas of focus in the field of autonomous vehicles [1]. Regarding the specific area of Articulated Vehicles (AV) as the one depicted in Figure 1, their autonomous operation has received considerable attention from researchers lately such as in [2]. However, in most of the existing research approaches, the focus has been in the remote operation of the AVs rather than embedding autonomy into the vehicles for accomplishing specific missions in controlled environments [3]. Currently, there is a continuous trend for increasing the overall levels of AVs' autonomy, especially in the field of on-line path planning and in related control schemes.



Figure 1: Type of an articulated vehicle

10

The specific geometry of the AV is more suitable to a free space constrained environment, than a car-like vehicle [4]. Furthermore, an articulated vehicle is able to perform sharper turns from an Ackerman vehicle of a similar length, while it is being characterised in general by a higher manoeuvrability [5] and thus AVs are commonly found in multiple applications in the fields of mining and construction sites [6].

Regarding the area of path planning, one of the major challenges is to satisfy the vehicle's kinematic constraints, while applying the generated planned path, a problem that to the authors best knowledge is still an open research issue. Towards this direction, common and rather oversimplified and non-realistic approaches have been the cases where the vehicle has been considered as a unit point, with the major kinematics of the vehicle neglected for simplicity reasons, while the AV has been considered of having full translation capabilities with a general state space representation of $\dot{x} = u$, with u the actuating control signal.

20

For a path planning approach compatible with the vehicle's constraints, a non-
25 holonomic path planning method, for minimizing the traveling length and curvature
constraints, has been presented in [7], while in [8] it has been investigated the utiliza-
tion of polar polynomial curves to produce a continuous path changing, under specific
curvature constraints. In [9, 10, 11] extensive work focusing on the systematic error to
achieve minimal path planning errors has been evaluated, while in [12] an algorithm
30 for minimizing the maximum path length in real time has been presented. Furthermore,
in [13], a new scheme based on calibration equations, introducing fewer approximation
errors in order to reduce kinematic modeling errors, was proposed.

From a control point of view, there have been proposed many traditional techniques
for nonholonomic vehicles, based on error dynamics models without the presence of
35 slip angles. A control scheme that combines a kinematic and a sliding mode controller
for wheeled mobile robots has been presented in [14, 15]. In [16] a general kinematic
model of an articulated vehicle has been proposed that described how heading angle
evolved with time as a function of steering angle and velocity. In [17] a Lyapunov based
approach has been presented that addressed the problem of asymptotic stabilization for
40 backward motion. A nonlinear control law based on partial state feedback linearization
and a Lyapunov method for the closed-loop path following problem of a nonholonomic
mobile robot has been appeared in [18, 19]. Finally, a control scheme based on linear
matrix inequalities has been presented in [20] and in [21] a pole placement technique
has been applied.

45 The main contributions of this article are the following ones. Firstly, a modified
novel Bug like algorithm will be coupled with the MPC in order to establish a smooth
and efficient path planning scheme for an AV. The proposed scheme is based on a partial
sensory-based awareness of the AV's surrounding environment and a priori knowledge
about the current goal points. Secondly, the full kinematics of the vehicle and especially
50 its non-linearities will be considered in the proposed online path planning algorithm.
Thirdly, a sensitivity analysis of the proposed combined online path planning and MPC
scheme will be presented.

The rest of the article is organized as follows. In Section 2, the AV kinematic
and error dynamics models are being presented, while in Section 3, the proposed on-

55 line path planning is being demonstrated in combination to the utilized MPC scheme. In Section 4, multiple simulation results, subjected to various conditions, are being analyzed examining the sensitivity of the proposed scheme, while proving the overall efficacy in different arenas and in different configurations. Finally, the concluding remarks are provided in Section 5

60 2. Articulated Vehicle And Error Dynamic Models

The AV's geometry is represented in Fig.2. It consists of two parts, a front and a rear, with lengths l_1 and l_2 respectively, linked by a rigid free joint, while the overall vehicle's width is denoted by w . Each body has a single axle and all wheels are non-steerable. The centers of gravity for these parts are being denoted as $P_1 = (x_1, y_1)$ and
65 $P_2 = (x_2, y_2)$. The steering action is being performed on the center joint, by changing the corresponding articulated angle γ . Furthermore, the velocities v_1 and v_2 are considered to have the same change, with respect to the velocity of the rigid free joint of the vehicle, while C is the instantaneous center velocity of the front and rear parts with different radiuses (r_1, r_2). For the described non-holonomic AV, the kinematic
70 model, including the vehicle's configuration has been extendedly introduced and analyzed in [22]. This kinematic model deals with the geometric relationships between the

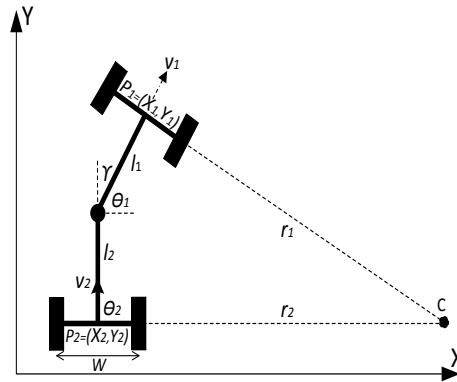


Figure 2: Articulated vehicle's geometry.

control parameters and the overall behaviour of the vehicle, while it has been assumed

that the vehicle is traveling forward without slip, by controlling the rate change of the steering angle $\dot{\gamma}$. The non-holonomic constraints acting on the front and rear axles, can
75 be expressed as it follows:

$$\dot{x}_1 \sin \theta_1 - \dot{y}_1 \cos \theta_1 = 0 \quad (1)$$

$$\dot{x}_2 \sin \theta_2 - \dot{y}_2 \cos \theta_2 = 0 \quad (2)$$

For deriving the vehicle's kinematic equations, it is assumed that a) the steering angle γ remains constant under small displacements, b) the dynamical effects due to low speed (like tire characteristic, friction, load and breaking force) are being neglected, c) each axle is being composed of two wheels that can be replaced by a unique wheel, and d)
80 the vehicle moves on a plane without slipping effects. Furthermore, it is assumed that the vehicle's velocity is bounded within the maximum allowed velocity, which prevents the vehicle from slipping. From the geometrical characteristics of the vehicle it can be easily derived that the equations describing the translation of the articulated front part are:

$$\dot{x}_1 = v_1 \cos \theta_1 \quad (3)$$

$$\dot{y}_1 = v_1 \sin \theta_1 \quad (4)$$

85 The velocities v_1 and v_2 are considered to have the same changing with respect to the velocity of the rigid free joint of the vehicle and thus the relative velocity vector equations can be defined as:

$$v_1 = v_2 \cos \gamma + \dot{\theta}_2 l_2 \sin \gamma \quad (5)$$

$$v_2 \sin \gamma = \dot{\theta}_1 l_1 + \dot{\theta}_2 l_2 \cos \gamma \quad (6)$$

where $\dot{\theta}_1$ and $\dot{\theta}_2$ are the angular velocities of the front and rear parts respectively. Combining equations (5) and (6) yields:

$$\dot{\theta}_1 = \frac{v_1 \sin \gamma + l_2 \dot{\gamma}}{l_1 \cos \gamma + l_2} \quad (7)$$

90 For the case that there is a steering limitation for driving the rear part according to the coordinates of the point (x_2, y_2) , the relationship between front and rear coordinates is

provided by:

$$x_2 = x_1 - l_1 \cos \theta_1 - l_2 \cos \theta_2 \quad (8)$$

$$y_2 = y_1 - l_1 \sin \theta_1 - l_2 \sin \theta_2 \quad (9)$$

Based on the full modelling approach presented in [22] and from (3), (4), and (7) the state space vector for the AV is defined as $\mathbf{x} = [x_1 \ y_1 \ \theta_1 \ \gamma]^T$, with the following

95 kinematic model representation for the front part:

$$\begin{bmatrix} \dot{x}_1 \\ \dot{y}_1 \\ \dot{\theta}_1 \\ \dot{\gamma} \end{bmatrix} = \begin{bmatrix} \cos \theta_1 & 0 \\ \sin \theta_1 & 0 \\ \frac{\sin \gamma}{l_1 \cos \gamma + l_2} & \frac{l_2}{l_1 \cos \gamma + l_2} \\ 0 & 1 \end{bmatrix} \begin{bmatrix} v \\ \dot{\theta}_\gamma \end{bmatrix} \quad (10)$$

where $\dot{\theta}_\gamma$ is the rate of change for the articulated angle, denoted also as $\dot{\gamma}$. As it has been extensively presented in [23], the system representation can be formulated as a set of error dynamic equations. These error dynamics are described by the following parameters depicted in Fig.3, which are the curvature e_c , the heading e_h , and the displacement e_d errors. In the presented error dynamics approach, the e_c is the difference between the curvature of the desired and the actual path. The e_h is the angle between the centers of the desired and actual path, when considering the front center of the vehicle. Finally, the e_d is the difference between the two paths with respect to the vehicle's location. The curvature error can be presented using the equation $e_c = (1/r - 1/R)$.

105 By assuming that the vehicle velocity v and the radius of the reference path R are constant, then; $\dot{e}_c = d(\frac{v \sin \gamma + l_2 \dot{\gamma}}{v(l_2 + l_1 \cos \gamma)})/dt$. Furthermore, the rate of the curvature error is being defined as:

$$\dot{e}_c = \dot{\gamma} \frac{l_2 \cos \gamma + l_1}{(l_1 \cos \gamma + l_2)^2} + \ddot{\gamma} \frac{l_2 (l_1 \cos \gamma + l_2)}{v(l_1 \cos \gamma + l_2)^2} - \dot{\gamma}^2 \frac{l_1 l_2 \sin \gamma}{v(l_1 \cos \gamma + l_2)^2} \quad (11)$$

As defined in Fig.3, the change of heading error is: $e_h = \theta_1(1 - \frac{r}{R})$, by utilizing the relations ($r = \frac{v}{\dot{\theta}}$) and $e_c = (\frac{1}{r} - \frac{1}{R})$, the rate of heading error is being calculated as:

$$\dot{e}_h = v e_c + \dot{\gamma} \frac{l_2}{l_1 \cos \gamma + l_2} \quad (12)$$

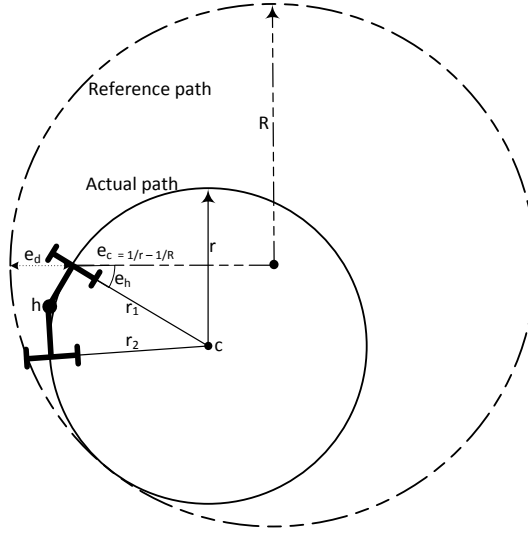


Figure 3: A graphical representation of the error dynamics transformation.

110 The displacement error is being defined as: $e_d = r\theta e_h - l_1 \cos \gamma$ and by taking the time derivative of this equation it can be derived that:

$$\dot{e}_d = v e_h + \dot{\gamma} l_1 \sin \gamma \quad (13)$$

By linearizing the error dynamics in the equations (11), (12) and (13) around the reference path and by considering small changes in the articulated angle, measured in radians, and by redefining the state variables into a form containing a single control input (the rate of the articulation angle) it yields into [23]:

115

$$\begin{bmatrix} \dot{e}_c \\ \dot{e}_h \\ \dot{e}_d \end{bmatrix} = \begin{bmatrix} 0 & 0 & 0 \\ v & 0 & 0 \\ 0 & v & 0 \end{bmatrix} \begin{bmatrix} e_c \\ e_h \\ e_d \end{bmatrix} + \begin{bmatrix} k_1 \\ k_2 \\ 0 \end{bmatrix} \dot{\gamma} \quad (14)$$

where $k_1 = \frac{1}{l_1+l_2}$ and $k_2 = \frac{l_2}{l_1+l_2}$ are constants and the derivative of the error states vector can be further denoted by $\dot{\mathbf{x}}_e = [\dot{e}_c \ \dot{e}_h \ \dot{e}_d]^T$. This error dynamics model in Eq. (14) is going to be utilised in the sequel for developing the proposed path planning algorithm and the corresponding MPC scheme for the AV's motion planning.

120 **3. Path Planning and Motion Control**

As it has been mentioned before, in the related literature of AV's and especially in the area of path planning, the vehicle is being modeled as a unit dynamics point and this approach is mainly due to simplicity and for avoiding the non-linearities of the AV model. However, one of the contributions of this article is to present an over-
125 all and complete motion planning approach for an AV, based on the full kinematics of the vehicle, combine it with a MPC scheme, evaluate the performance of the motion planning algorithm in more realistic scenarios and present an extended analysis of the algorithms sensitivity based on numerous simulation results, while extending and strengthening the results presented in [24]. The sensitivity analysis, which will be
130 presented in the next Section is considered as the most important contribution of this article since instead of providing a couple of simulation results, it evaluates the presented scheme from an extended point of view based on multiple simulation results and based on significant algorithmic parameters that dramatically effect the performance of the proposed scheme, while providing direct insights and discussions. However, before
135 the sensitivity analysis, the complete and extended approach on the motion planning, which includes the steps of path planning and path tracking will be presented in this Section.

3.1. Modified Path Planning

The proposed online path planning algorithm can be applied for the objective of
140 moving a vehicle from a starting point to the goal point, while detecting and avoiding identified obstacles based on the real vehicle's dynamic equations of motion and the Model Predictive Controller. As a common property of the Bug like algorithms, the proposed scheme initially faces the vehicle towards the assumed constantly known goal point. In the presented algorithm, it has also been assumed that the vehicle is
145 able to on-line sense the surrounding environment, included in a sensing radius of r_{obs} . During translation, the path planner is on-line generating future way points that act as a reference path for the utilized MP-controller. Before feeding the MPC with the reference coordinates, a proper conversion is taking place from the Cartesian space to the

curvature, heading and distance space, which consist the states of the vehicle's error
 150 dynamic model [23]. The overall proposed concept of path planning and MPC control
 is depicted in Figure 4. As it can be observed from this diagram, the algorithm starts by

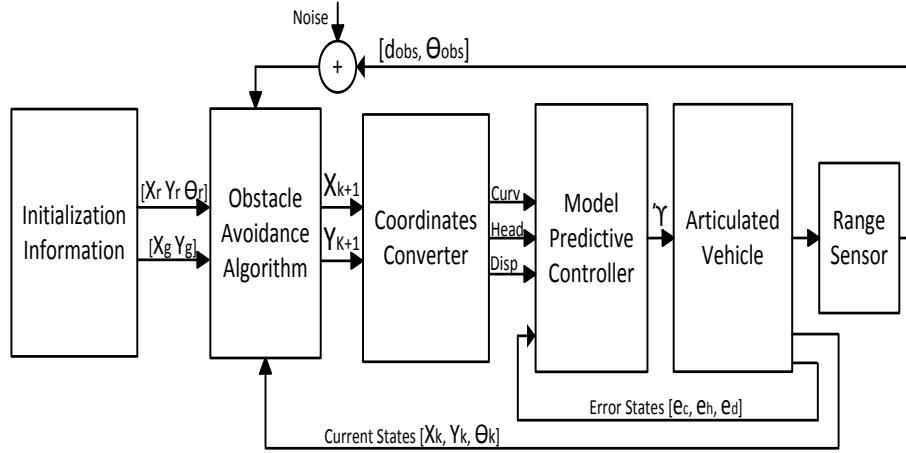


Figure 4: The combined on-line path planning and MPC for the AV

defining the current position and orientation of the vehicle, denoted by $[X_r, Y_r, \theta_r]$ and
 the final goal position denoted by $[X_g, Y_g, \theta_g]$. Based on the onboard sensory system,
 the vehicle identifies the surrounding environment and obstacles and generates on-line
 155 the way points for reaching the goal destination, by solving the local and by definition
 sub-optimal, path planning problem. In the sequel the way points are been translated to
 references for the error dynamics based MP controller. The control scheme generates
 the rate of articulated angle, which is the control signal for the vehicle. In the pre-
 sented architecture, it is assumed that accurate and continuous position and orientation
 160 measurements as well as corresponding updates are being provided, without any loss
 of generality.

The assumed sensory system is able to provide a partially bounded information on
 the surrounding environment due to the assumption of a limited sensing range $r_{obs} \in \mathfrak{R}$,
 while these measurements are being transformed to relative distances and angles from
 165 the articulated robot to the identified surroundings or obstacles, defined as $d_{obs} \in \mathfrak{R}$
 and $\theta_{obs} \in \mathfrak{R}$ correspondingly. It should be noted that in the presented approach all

the obstacles and the surrounding environment are being considered as point clouds in a 2-dimensional space, while overlapping obstacles are being merged and represented by a single and unified obstacle. In the path derivation a safety distance has been also considered, denoted as $r_{min} \in \mathfrak{R}$, for protecting the vehicle from approaching close to the obstacles. In the consideration of this safety distance, the algorithm calculates the related distance and angle from the identified obstacle, denoted as $d_{min} \in \mathfrak{R}$ and $\theta_{min} \in \mathfrak{R}$, while tuning the path planning accordingly. The notations utilized and the overall concept of the proposed path planning algorithm are depicted in Figure 5. The operation and the sequential execution of the proposed path planning and control

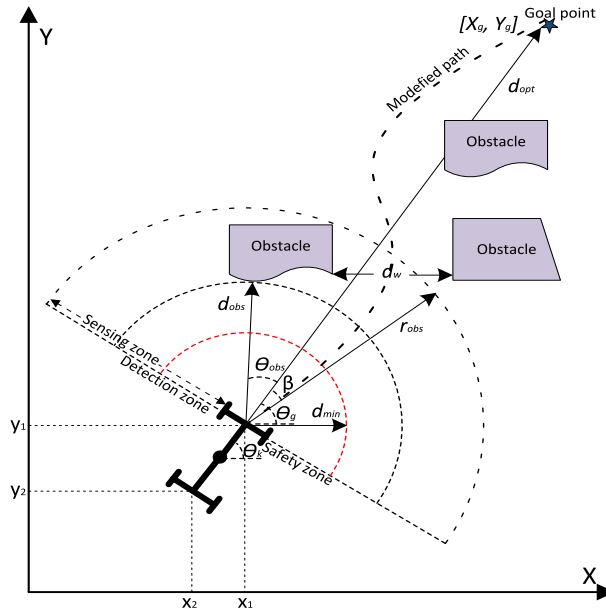


Figure 5: Notations and overall concept of the proposed online path planning algorithm

scheme can be summarized as it is depicted in the following table, while in [24] a full analysis of the presented approach can be found:

3.2. Model Predictive Control

The proposed MPC is utilizing the state space representation (14) for generating the proper rate of articulation angle for controlling the articulated vehicle. In order

Path Planning Algorithm

Initialization

- Set parameters: $[X_k \ Y_k \ \theta_k]$, $[X_g \ Y_g]$ and $[v, \dot{\gamma}, d_{min}, \theta_{min}, r_{min}, d_{obs}, \theta_{obs}, T]$.

Path Update

- Calculate orientation to the goal $\theta_g(k) = \arctan \frac{Y_g - Y_k}{X_g - X_k}$ and the difference angle $\beta(k) = \theta_g(k) - \theta_k$

Goal Update

- Update, $x(k) = v \cos(\theta(k) + \beta(k))$, $y(k) = v \sin(\theta(k) + \beta(k))$, and $\theta(k) = \beta(k)$

Scan Area

- Compute smallest distance, $d_{obs} = \sqrt{(X_{k+1} - X_{obs})^2 + (Y_{k+1} - Y_{obs})^2}$
- Compute angle to the obstacle, $\theta_{obs} = \arctan \frac{Y_{k+1} - Y_{obs}}{X_{k+1} - X_{obs}}$
- Compute angle between the obstacle and the goal, $\theta_{obs,g} = \theta_{obs} - \theta_g$

Obstacle Detection

- Evaluate the risk of collision, $(d_{obs} < d_{min})$ AND $(\theta_{obs,g} < \theta_{min})$
- Evaluate the angle to the obstacle, $(d_{obs} < d_{min})$ AND $(\theta_{obs} < -\theta_{min}, \theta_{obs} > \theta_{min})$

Obstacle Avoidance Conditions

- If being satisfied, $\theta_{obs,g} > 0$: $\beta(k+1) = \beta(k) + \Delta\beta(k)$, and if, $\theta_{obs,g} < 0$: $\beta(k+1) = \beta(k) - \Delta\beta(k)$

Update Reference Path for MPC

- Update, $x(k+1) = x(k) + v \cos(\beta(k+1))$, and update, $y(k+1) = y(k) + v \sin(\beta(k+1))$

Algorithm Termination

- If, $x(k+1) \in X_g \pm T$ AND $y(k+1) > Y_g \pm T$
- Go To Step "Path Update"

Otherwise

- Vehicle Reaches Goal and Velocity = 0
-

to design the MPC controller for path following, the linearized system (14) will be discretized as:

$$\mathbf{x}_e(k+1) = A\mathbf{x}_e(k) + Bu_e(k) \quad (15)$$

where $A \in \mathbb{R}^n \times \mathbb{R}^n$, n is the number of state variables and $B \in \mathbb{R}^m \times \mathbb{R}^m$, m is the number of input control variable, x_e is the error dynamics state vector and with u_e is the control signal (the rate of the articulated angle). The overall aim of the MPC is to calculate a proper control signal that minimizes the quadratic objective function of the states and control input with predictive horizon M , which is being described by:

$$J(k) = \sum_{j=1}^M (\mathbf{x}_e^T(k+j|k)Q\mathbf{x}_e(k+j|k)) + \sum_{j=1}^N (\mathbf{u}_e^T(k+j-1|k)R\mathbf{u}_e(k+j-1|k)) \quad (16)$$

where $Q \in \mathbb{R}^n \times \mathbb{R}^n$ is the weighting matrix for predicted errors and $R \in \mathbb{R}^m \times \mathbb{R}^m$ is the weighting matrix for control input. The Q and R weighting matrices are positive diagonal matrices with largest elements corresponding to the most important variables, while an increase in the values of weights tends to make the MPC controller more conservative. In the presented approach, the widely utilized ad-hoc tuning procedure for these weights have been followed in order to optimize the simulated results obtained. Finally, the control action is being obtained by solving on-line the optimization $J(k)$ with respect to the control variation Δu and the errors coordinates.

To handle the state and input constraints, let the bounds in the states variables as the following bounding inequality:

$$\mathbf{x}^{min} = \mathbf{x} - \Delta_1 \leq \mathbf{x} \leq \mathbf{x} + \Delta_1 = \mathbf{x}^{max} \quad (17)$$

where $\Delta_1 \in \mathbb{R}^n \times \mathbb{R}^n$ is the vector containing the selecting state boundary conditions, which are the maximum and minimum allowable limits for AV's error dynamics. Furthermore, the control input bounds could be derived by taking under consideration the mechanical and physical constraints of the articulated steering angle, while these constraints can be formulated as:

$$u^{min} = u - \Delta_2 \leq u \leq u + \Delta_2 = u^{max} \quad (18)$$

where $\Delta_2 \in \mathbb{R}^m \times \mathbb{R}^m$ is the vector containing the selecting control boundary condition. These constraints are embedded in the MPC computing algorithm in order to compute

205 an optimal controller that counts for the constraints that restrict the articulated vehicle's motion.

During the deviation of the MPC, special care should be provided in order to correctly tune the prediction M and the control N horizons. A long prediction horizon increases the predictive ability of the MPC controller but on the contrary it decreases
210 the performance and demands more computations. The control horizon must also be fine-tuned since a short control horizon leads to a controller that tries to reach the setpoint with a few conservative motions, a method that might lead to significant overshoots. On the contrary, a long control horizon produces more aggressive changes in the control action that tend to lead to oscillations. Obviously the tuning of prediction
215 and control horizon is a coupled process. For the aforementioned reasons the control horizon must be chosen short enough compared to the prediction horizon. Additionally, the response of the system can be also shaped using weight matrices on the system outputs, the control action and the control rates.

4. Simulation Results

220 For simulating the efficacy of the proposed path planner and evaluating its sensitivity against the motion parameters, the following AV's characteristics have been considered as: $l_1 = l_2 = 0.61m$, $w = 0.58m$, while the vehicle's velocity for this part of simulation is in the range of $(0.5 \leq v \leq 2)m/sec$. Moreover, the constraints imposed on the articulated angle γ have been defined as: $-30^\circ \leq \gamma \leq +30^\circ$ and random measurement Gaussian noise with a fixed variance has been added to the measurements of
225 the range sensor to simulate the real-life distortion. The parameters of the MPC have been tuned as: a) prediction horizon (number of predictions) $M = 10$, b) control horizon (number of future control moves) $N = 5$, and c) a time sampling period of $0.2 sec$. The constraints imposed on the input and control weighting matrices have been tuned
230 according to the current active state space model as: weighting matrix for predicted errors $Q = 0.3I_{3 \times 3}$ and weighting matrix for control movement $R = 0.1$ for suspending aggressive manoeuvres. In the presented simulation results additional corrupting noise for the feedback range sensors signals has been considered to add more realistic behav-

ior. This white noise has a a uniform distribution and a gain of 0.01 to simulate the real
 235 life measurement distortion and has been tuned based on our real life experience and
 experimentation with the utilized range sensors (ultrasound sensors).

In Fig.6, a typical example of the AV's motion behavior in an open-loop configura-
 tion is being presented. The simulation of the non-linear model has been performed
 by considering the AV to start translating from a start point of $[x = 20, y = 20, \theta =$
 240 $0, \gamma = -10^\circ]$, while $\dot{\gamma}$ is changing with respect to time, in positive and negative orien-
 tations. The case of movement from a starting point into two different goal points, in

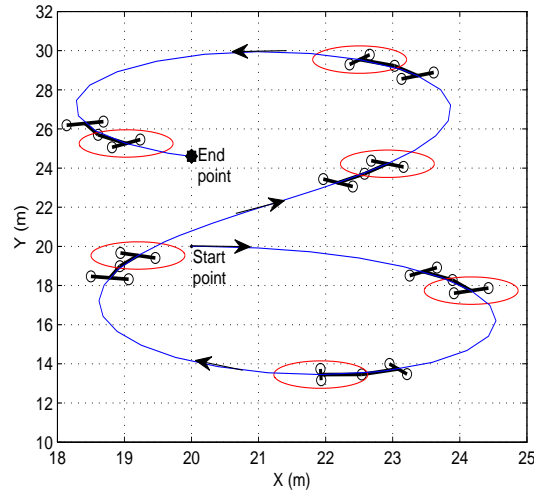


Figure 6: Motion behavior of the AV (8-pattern).

an arena with differently shaped obstacles, is being considered in Fig.7. In this case,
 the AV's states initiate from $[0 \ 0 \ 45^\circ \ 7.5^\circ]$ and the multiple distinct goal points have
 been set as $[10, 35]$ and $[20, 25]$ respectively, with $r_{obs} = 4m$ and $d_{min} = 3$. In
 245 the depicted closed loop paths, the articulated kinematics of the vehicle are obvious due
 to the existing curvature of the vehicle during translation. Furthermore, in Fig.8 the
 corresponding responses of the error dynamics states, as well as the articulated angle
 and the rate of the angle (control effort) are being depicted for both examined path
 tracking scenarios, (blue-lines for Goal point 1 and red-dashed lines for Goal point 2).

In the second scenario, the case of movement within a multiple bounding surrounding

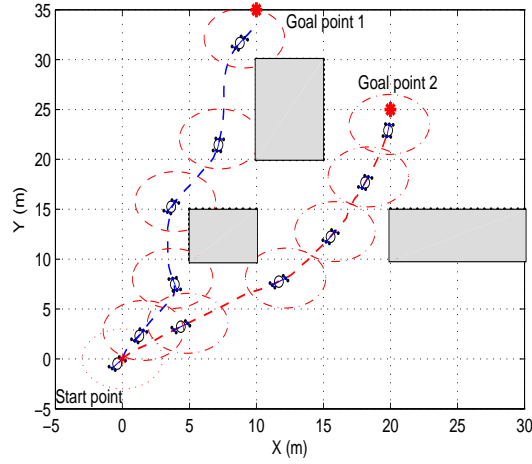


Figure 7: Path tracking in an open arena with different shape obstacles.

250

environment is being considered, as presented in Fig.9, which mimics the operation in a mining environment or a construction site. In the examined case, the AV starts at $[0 \ 0 \ 15^\circ \ 7.5^\circ]$ with the goal points (1,2,3) at $[10 \ 15]$, $[40 \ 10]$, and $[10 \ -15]$, respectively, with $r_{obs} = 3m$ and $d_{min} = 2$. As in the previously examined case, the proposed scheme manages to provide smooth path generation and tracking for the vehicle. The existence of non-holonomic behaviour, due to the articulated dynamics, is again obvious due to the curvature of the obtained path. The corresponding responses of the error dynamics states, as well, the articulated angle and the rate of the angle (control effort), which are being depicted for only the case of path generation and tracking to the second goal point are being presented in Fig.10. In the sequel the sensitivity of the proposed scheme will be evaluated with respect to the corresponding Kinematic Parameters (KP) defined by the vehicle's velocity v , the maximum allowable change in the steering angle $\Delta\beta$ suggested by the path planner, the safety distance d_{min} and the overall number of obstacles in a fixed size arena. The arenas that are going to be considered are: a) an open area with dimensions $(15 \times 15)m$, with 9-obstacles in fixed locations and b) an open area with dimensions $(35 \times 35)m$ and with a random number,

265

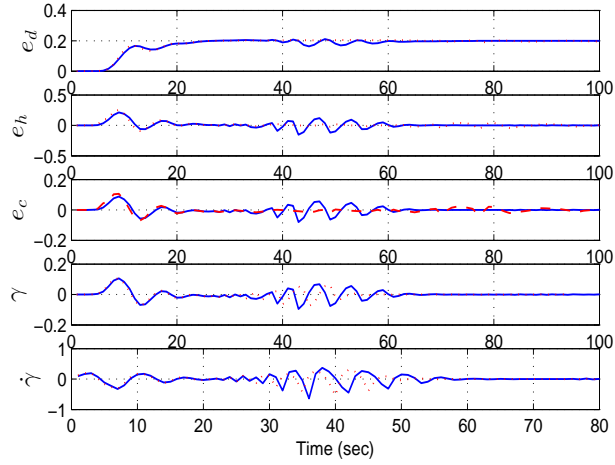


Figure 8: Vehicle's error dynamics response and corresponding articulated angle γ and MPC's effort $\dot{\gamma}$.

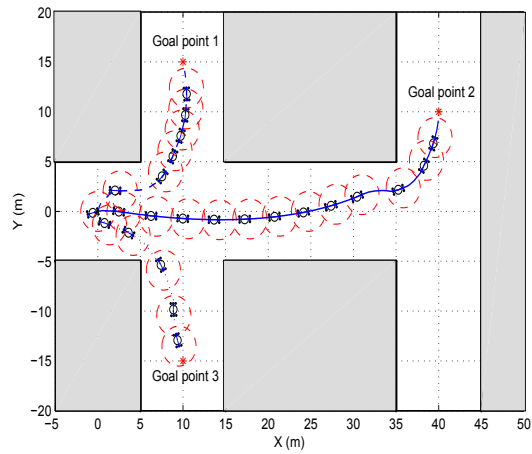


Figure 9: The arena having same boundaries on both sides of the road.

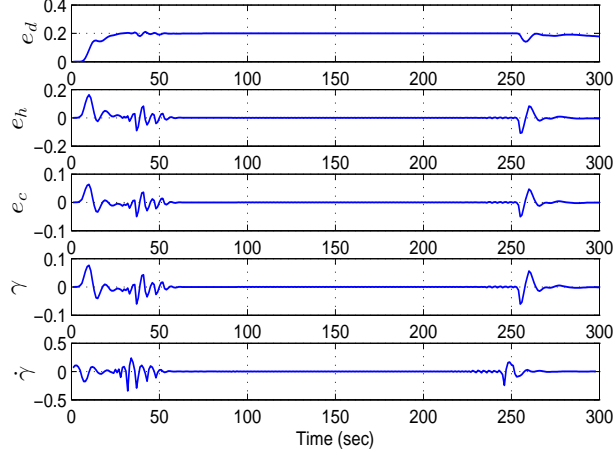


Figure 10: The systems states error dynamics performance in meter, for the case of path generation and tracking to the second goal point.

(0 – 400) or 0 – 200, and positioning of fixed size obstacles. In all the examined test cases, the obstacles are of a squared shape with sides of (1m). The aim of the proposed on-line path planning scheme was to generate a collision free path, from the initial posture to the destination point. The previous selected KP are the ones that could be tuned and have a direct effect on the overall maneuverability of the AV. In all the simulated test cases, an important efficiency indicator will be the AV’s length of route or translated distance (m), during the translation from the initial posture to the final one.

In the beginning of the sensitivity analysis, the case of having a fixed $\beta = 12deg$ and with varying d_{min} and v is being considered for the case of an open area with 9 fixed obstacles. In this case the AV starts from an initial point of [0 0 10 7.5] and with a final goal point at [15 15], while no demand on the orientation, when reaching the goal point has been set. The obtained simulated results are being depicted in Figure 11, while for comparison reasons, it should be stated that the shortest distance in this problem is the straight, and free of obstacles, path of 21.2m. During the described simulations, the variation of the KP has been set as $0.5 \leq v \leq 2m/s$ with a step change of 0.1m/s and $0.5 \leq d_{min} \leq 2m$ with a step change of 0.1m. In the presented results, when the traveling

distance is equal to $0m$ it indicates that the AV failed in reaching the desired end goal, with the selected KP configuration. From the obtained results in Fig.11 it is obvious

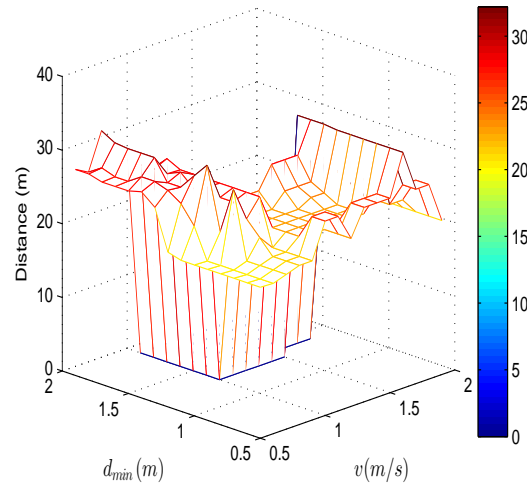


Figure 11: Successful reaching of the final goal and overall distance traveled under constant allowable change of path planner's steering angle and varying speed and safety distance (open area with 9 fixed obstacles).

285 that in general low-velocities and smaller safety distances can achieve an accurate and short-distanced path to reach the goal point, while in the examined scenario, from the 225 iterations, only 64 cases failed to reach the indicated target goal.

In Figure 12, the case of fixing the velocity at $v = 1m/s$ and having the rest of KP varying as $10 \leq \beta \leq 25deg$, with a step change of $1deg$ and $0.5 \leq d_{min} \leq 2m$ with a step change of $0.1m$ is being presented. As it has been indicated from the
 290 obtained simulation results, at small safety distances, the allowable changing of the steering angle has the same effect during the movement towards the goal position. In these simulations, 68 cases out of in total 225 iterations have failed in reaching the target goal. However, in contrast to the previous test case, it should be highlighted
 295 that in general the constraint on the steering angle is not so significant on the AV's steering responses under a constant velocity and small safety distances. In Fig.13,

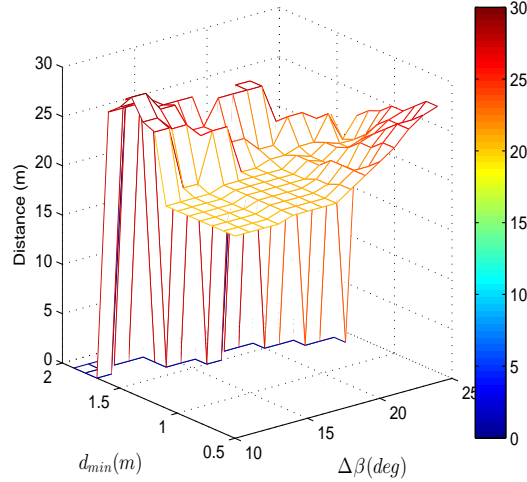


Figure 12: Successful reaching of the final goal and overall distance traveled under constant speed and varying allowable change of the path planner's steering angle and speed (open area with 9 fixed obstacles).

the final case for the first scenario has been considered, where d_{min} has been fixed at $1.2m$ and the rest of the KP are considered varying as $10 \leq \beta \leq 25 \text{ deg}$, with a step change of 1 deg and $0.5 \leq v \leq 2 \text{ m/s}$ with a step change of 0.1 m/s . The obtained

300 results indicate that the combination of a small rate for the steering angle with high velocities are sufficient proper for reaching the goal point at short distances. Overall, in these simulated test cases, there have been in total 27 failed cases out of the total 255. As a general outcome, from the obtained sensitivity results, in order to increase the performance of the proposed on-line path planning and control scheme and allow

305 the vehicle to reach the goal point successfully, it is better to travel at low velocities and at smaller safety distances, for avoiding the collision with obstacles, while normal (mean value) for the rate in the articulation angle are being suggested. As illustrative examples, from the presented analysis, in Fig. 14 the AV motion is being displayed under a fixed low-velocity of ($v = 0.5 \text{ m/s}$), a fixed allowable change in the steering angle of ($\gamma = 12 \text{ deg}$) and in four cases with a different range of safety distance as:

310

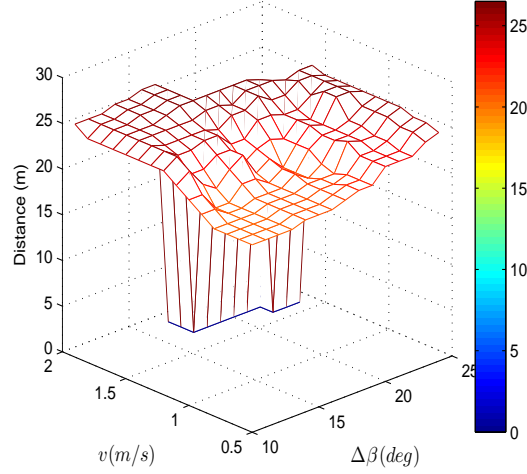


Figure 13: Successful reaching of the final goal and overall distance traveled under constant safety distance and varying allowable change of the path planner’s steering angle and safety distance (open area with 9 fixed obstacles).

case-a ($d_{min} = 0.5$), case-b ($d_{min} = 1.0$), case-c ($d_{min} = 1.5$), and case-d ($d_{min} = 2.0$). From the obtained results it is obvious that in the cases-a and b the AV can reach the goal at the location [15 15] in a shortest traveling distance. In case-c, the AV reaches the goal point with a longer distance, while case-d could not reach the goal point. In the sequel the sensitivity of the proposed scheme will be evaluated in the scenario of an open area being populated by moving and varying number of obstacles. As in the previous case, the cases of having varying β , d_{min} and v with respect to a varying number of obstacles will be considered. In this case the vehicle again starts from an initial point of [0 0 10 7.5] and with a final goal point at [15 15], while no demand on the orientation, when reaching the goal point has been set.

For the first simulation, the case of having a varying speed and varying number of obstacles will be considered. The obtained results are being depicted in Figure 15 with a corresponding variation of $0.5 \leq v \leq 2m/s$ and with a step change of $0.1m/s$, while the number of obstacles is between 0-400. From the simulated results it is obvious that

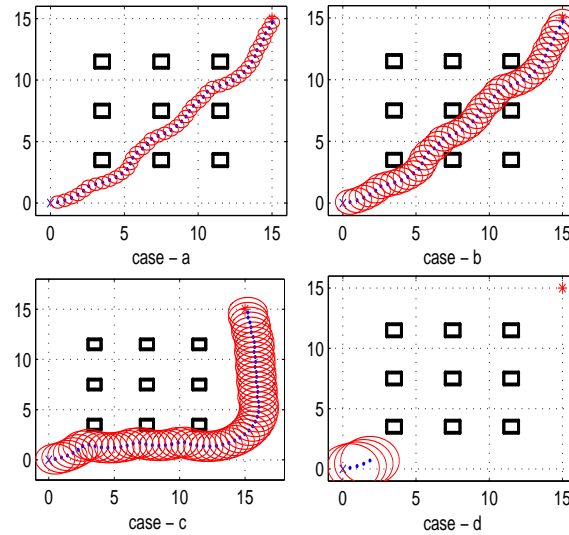


Figure 14: Illustrative examples from the scenarios in the arena with fixed obstacles

325 the speed is of paramount importance, especially in the cases with a high number of
 obstacles. For speeds higher than $1.5m/s$ the proposed algorithm cannot reach the end
 goal, while for lower speeds the performance of the path planning is satisfactory. In the
 presented results there have been in total 122 out of 400 iterations where the proposed
 on-line path planner did not achieve to reach the final goal. At this point it should be
 330 highlighted again that this simulations concern the on-line and closed loop (MPC) path
 planning, incorporating the full kinematic constraints of the AV. In case that the safe
 distance is being considered with respect to the varying number of obstacles, the results
 are being depicted in 16. From the obtained results is is obvious that smaller safety dis-
 tances are creating more flexibility to the AV and prevents it from falling into local
 335 minimums, while large safety distances, in combination with an increased number of
 obstacles are causing the proposed scheme to fail. In the presented results there have
 been in total 56 out of 255 iterations where the proposed on-line path planner did not
 achieve to reach the final goal. In the last case, the maximum allowable change in path
 planner's articulation angle is being considered with respect to the varying number of
 340 obstacles, while the results are being depicted in Figure 17. From the obtained results

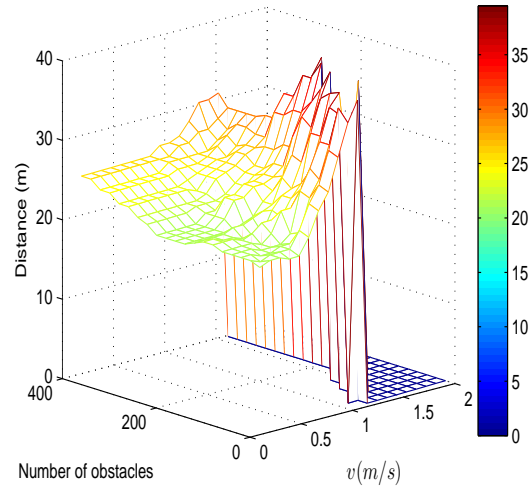


Figure 15: Successful reaching of the final goal and overall distance traveled under varying speed and number of obstacles

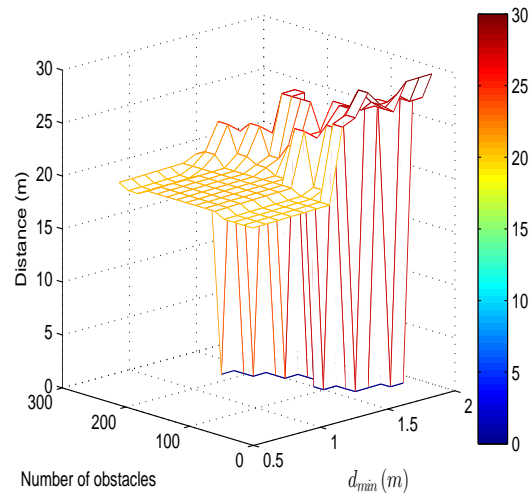


Figure 16: Successful reaching of the final goal and overall distance traveled under varying safety distance and number of obstacles

is has been indicated that the proposed scheme operates with a very good performance, as long as the number of obstacles remain bellow 200 and the allowable change of the articulation is limited up to $20deg$. For a bigger number of obstacles, the space is populated in an extremely dense manner and thus the AV is arriving into local minimums, independently of the allowable change of the articulation angle. In the presented results there have been in total 22 out of 255 iterations where the proposed on-line path planner did not achieve to reach the final goal. As an illustrative example from the presented

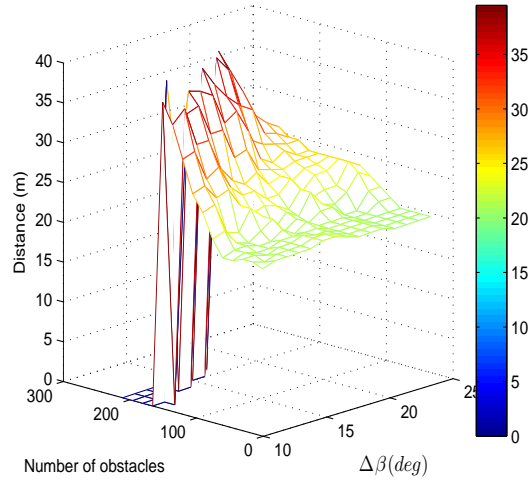


Figure 17: Successful reaching of the final goal and overall distance traveled under varying allowable change in the path planner’s suggested articulated angle and number of obstacles.

analysis, in Figure 18 the AV motion is being displayed with $v = 0.4m/s$, $\beta = 12deg/s$, and a safety distance of $1m$, in a geographically bounded area of $50 \times 50m$ and with 50, 100, 150 and 200 randomly positioned obstacles.

5. Conclusions

In this article the effect of kinematic parameters on a novel proposed on-line motion planning algorithm for an articulated vehicle based on Model Predictive Control

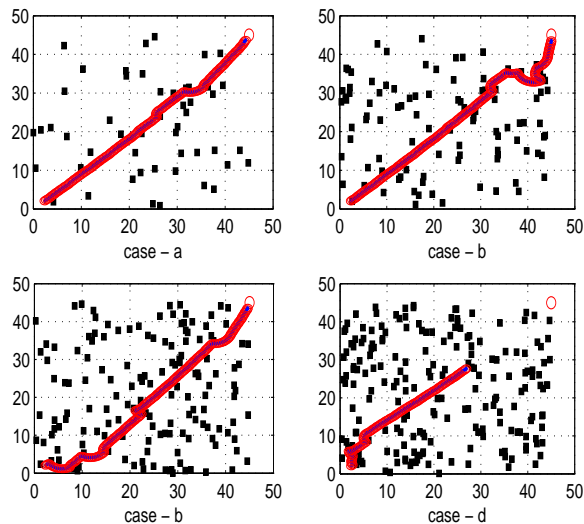


Figure 18: Indicative On-line path planning in a geographically bounded arena of $(50 \times 50)m$ with the following selection of KP: $v = 0.4m/s$, $\beta = 12deg$, and $d_{min} = 1m$ for the cases of: (a) 50, (b) 100, (c) 150, and (d) 200 obstacles.

(MPC) have been presented. The kinematic parameters that were considered have been
 355 the vehicle's velocity, the allowable change in the articulated angle from the path planner, the safety distance from the obstacles and the total number of obstacles in the operating arena. The proposed modified motion planning algorithm, for the articulated vehicle belonged to the family of Bug-Like algorithms and was able to take under consideration, the mechanical and physical constraints of the articulated vehicle, as well
 360 as its full kinematic model. The efficiency and the sensitivity of the proposed combined path planning and control scheme has been evaluated under numerous simulated test cases, while the dependencies to the selected kinematic parameters have been indicated.

References

- 365 [1] D. Katić, A. Ćosić, M. Šušić, S. Graovac, An integrated approach for intelligent path planning and control of mobile robot in structured environment, in: New

Trends in Medical and Service Robots, Springer, 2014, pp. 161–176.

- [2] R. Siegwart, I. R. Nourbakhsh, D. Scaramuzza, Introduction to autonomous mobile robots, MIT press, 2011.
- 370 [3] L. S. Martins-Filho, E. E. Macau, Trajectory planning for surveillance missions of mobile robots, in: Autonomous Robots and Agents, Springer, 2007, pp. 109–117.
- [4] S. M. LaValle, Motion planning, Robotics & Automation Magazine, IEEE 18 (2) (2011) 108–118.
- 375 [5] C. Altafini, Why to use an articulated vehicle in underground mining operations?, in: Robotics and Automation, 1999. Proceedings. 1999 IEEE International Conference on, Vol. 4, IEEE, 1999, pp. 3020–3025.
- [6] J. Roberts, E. Duff, P. Corke, P. Sikka, G. Winstanley, J. Cunningham, Autonomous control of underground mining vehicles using reactive navigation, in: Robotics and Automation, 2000. Proceedings. ICRA'00. IEEE International Conference on, Vol. 4, IEEE, 2000, pp. 3790–3795.
- 380 [7] T.-C. Liang, J.-S. Liu, G.-T. Hung, Y.-Z. Chang, Practical and flexible path planning for car-like mobile robot using maximal-curvature cubic spiral, Robotics and Autonomous Systems 52 (4) (2005) 312–335.
- [8] S. S. Ge, X.-C. Lai, A. Al Mamun, Sensor-based path planning for nonholonomic mobile robots subject to dynamic constraints, Robotics and Autonomous Systems 55 (7) (2007) 513–526.
- 385 [9] K. Yoo, W. Chung, Convergence analysis of kinematic parameter calibration for a car-like mobile robot, in: Advanced Intelligent Mechatronics, 2009. AIM 2009. IEEE/ASME International Conference on, IEEE, 2009, pp. 740–745.
- 390 [10] K. Lee, W. Chung, K. Yoo, Kinematic parameter calibration of a car-like mobile robot to improve odometry accuracy, Mechatronics 20 (5) (2010) 582–595.

- [11] K. Lee, C. Jung, W. Chung, Accurate calibration of kinematic parameters for two wheel differential mobile robots, *Journal of mechanical science and technology* 25 (6) (2011) 1603–1611.
- 395 [12] M. Davoodi, M. Abedin, B. Banyassady, P. Khanteimouri, A. Mohades, An optimal algorithm for two robots path planning problem on the grid, *Robotics and Autonomous Systems* 61 (12) (2013) 1406–1414.
- [13] C. Jung, W. Chung, Calibration of kinematic parameters for two wheel differential mobile robots by using experimental heading errors, *International Journal of Advanced Robotic Systems* 8 (2011) 134–142.
- 400 [14] S. Scheduling, G. Dissanayake, E. M. Nebot, H. Durrant-Whyte, An experiment in autonomous navigation of an underground mining vehicle, *Robotics and Automation, IEEE Transactions on* 15 (1) (1999) 85–95.
- [15] N. Hung, J. S. Im, S.-K. Jeong, H.-K. Kim, S. B. Kim, Design of a sliding mode controller for an automatic guided vehicle and its implementation, *International Journal of Control, Automation and Systems* 8 (1) (2010) 81–90.
- 405 [16] P. I. Corke, P. Ridley, Steering kinematics for a center-articulated mobile robot, *Robotics and Automation, IEEE Transactions on* 17 (2) (2001) 215–218.
- [17] A. Astolfi, P. Bolzern, A. Locatelli, Path-tracking of a tractor-trailer vehicle along rectilinear and circular paths: a lyapunov-based approach.
- 410 [18] A. Tayebi, A. Rachid, Path following control law for an industrial mobile robot, in: *Control Applications, 1996.*, Proceedings of the 1996 IEEE International Conference on, IEEE, 1996, pp. 703–707.
- [19] C. Altafini, A. Speranzon, B. Wahlberg, A feedback control scheme for reversing a truck and trailer vehicle, *Robotics and Automation, IEEE Transactions on* 17 (6) (2001) 915–922.
- 415 [20] P. Bigras, P. Petrov, T. Wong, A lmi approach to feedback path control for an articulated mining vehicle, *Electronics Research*.

- 420 [21] P. Ridley, P. Corke, Load haul dump vehicle kinematics and control, *Journal of dynamic systems, measurement, and control* 125 (1) (2003) 54–59.
- [22] T. Nayl, G. Nikolakopoulos, T. Gustafsson, Kinematic modeling and simulation studies of a lhd vehicle under slip angles, in: *Computational Intelligence and Bioinformatics/755: Modelling, Identification, and Simulation*, ACTA Press, 2011.
- 425 [23] T. Nayl, G. Nikolakopoulos, T. Gustafsson, Switching model predictive control for an articulated vehicle under varying slip angle, in: *Control and Automation, 2012 20th Mediterranean Conference on*, IEEE, 2012, pp. 884–889.
- [24] T. Nayl, G. Nikolakopoulos, T. Gustafsson, On-line path planning for an articulated vehicle based on model predictive control, in: *Control Applications (CCA), 2013 IEEE International Conference on*, IEEE, 2013, pp. 772–777.
- 430